High Q factor Electrically Injected Green Micro Cavity

Yang Mei, Yan-Hui Chen, Lei-Ying Ying, Zhi-Wei Zheng, Hao Long, and Bao-Ping Zhang

***Abstract*—Green micro-cavity (MC) with a quality factor (Q) exceeding 6000 was demonstrated under current injection. The MC consists of two dielectric DBRs and InGaN/GaN quantum wells in between. To form a lateral optical confinement (LOC) structure, a low-index thin AlN layer was used to replace part of the p-GaN. The device showed multi-longitudinal mode emission, from 460 to 540 nm, and higher-order lateral confined modes were clearly observed. By optimizing the cavity fabrication processes and lateral optical confinement, the linewidth of resonant mode is as narrow as 0.082 nm, indicating a high Q value of 6039 in green spectral region. This is the highest value in electrically injected GaN-based MC to the best of our knowledge. In addition, 3D confined optical states were observed and studied via angle resolved measurement for the first time in an electrically injected GaN-based MC. The emission characteristics of devices as a function of cavity length, as well as the loss mechanism inside the cavity were also systematically analyzed.**

***Index Terms*—3D confined optical states, electrically injection, high Q factor, loss analyses, micro cavity.**

I. Introduction

HIGH Q factor MCs can strongly confine photons in small volumes and a strong light-matter interaction can be obtained, thus attracting much attention in various fields, including photonics [1]–[3], telecommunications [4], quantum information [5], and cavity quantum electrodynamics. GaN-based semiconductors, including those of GaN, AlN, InN and their mixed alloys, are featured with wide bandgap and tunable emission spectrum covering from ultraviolet to near infrared [6], [7]. Besides, GaN-based materials have high oscillator strength (usually 10 times higher than GaAs) and large exciton binding energies [8]. These properties suggest that GaN-based MC with a high Q factor is an ideal platform for not only high efficient practical optical-electronic devices [9], [10], but also fundamental researches concerning light-matter interaction and cavity quantum electrodynamic (CQED) effect up to room temperature [11]–[14]. For the applications mentioned above, optical resonators with high quality, or equivalently, a high Q factor, are required. The cavity Q factor, which is defined as the totally stored energy divided by the energy loss over one radian of the oscillating cycle (2π radian), is an important parameter to evaluate the quality of resonators [15], [16]. The high Q resonances mean that a lot of energy can be stored in the waveguide layer. Exploring the methods to increase the cavity Q factor has been one of the main research directions of semiconductor MC. The Q factor of silicon and GaAs based MCs at telecom range has reached a very high value, exceeding 1000000 [14]. For GaN-based MCs designed for shorter wavelengths, namely from the visible to the ultraviolet spectral range, the Q factor is much smaller due to the increased scattering loss and the inferior crystal quality. The Q factors of the state-of-the-art optically pumped GaN-based MCs are in the order of 10000, including the Q factor of $\sim$18000 in Fabry-Perot (FP) planar cavity [17, 18], $\sim$14000 in defective photonic crystal cavity [19], [20], and $\sim$10200 in micro-disk cavity based on whispering-gallery modes (WGMs) [21], [22]. However, it is much more difficult for their electrically injected counterparts to realize such a high Q factor. At present, the highest cavity Q factor of electrically injected GaN-based MCs are $\sim$3570 for planar cavity [23], $\sim$800 for photonic crystal cavity [24], and less than 1000 for WGM cavity [25]–[27]. Electrically injected MCs have a more complicated structure to realize the current injection. The possible damages caused by the complicated fabrication processes, as well as the doping of the membrane might increase the internal loss and degrade the cavity Q factor [28].

In this work, we report an electrically injected green GaN-based planar MC with a high Q factor of 6039 by optimizing the fabrication processes and introducing a LOC structure. Two dielectric DBRs with high reflectivity were utilized and a sputtered AlN layer was used to confine both injected current and optical field. The device showed an emission spectrum covering from 460 to 540 nm, and the linewidth of the resonating mode is as narrow as 0.082 nm, indicating a high Q factor of 6039 in the green spectral region. This is the highest value in electrically pumped GaN-based MCs to the best of our knowledge. The loss mechanism in the cavity and the emission characteristics of devices with different cavity lengths were systematically analyzed. 3D confined optical states inside the cavity were also observed and studied through angle-resolved measurement. Due to the 3D optical confinement structure, the dispersion of optical states in momentum space is much more different from the typical continuous parabolic curve in a 2D planar MC. The mode dispersion is split into a series of discrete modes at different

Q1

Manuscript received October 23, 2020; revised December 28, 2020 and January 16, 2021; accepted January 18, 2021. This work was supported in part by by the National Key Research and Development Program of China under Grant 2016YFB0400803, in part by Science Challenge Project under Grant TZ2016003, and in part by the National Natural Science Foundation of China under Grant 61704140. *(Corresponding author: Bao-Ping Zhang)*

The authors are with the Department of Microelectronics and Integrated Circuit, Laboratory of Micro/Nano-Optoelectronics, School of Electronic Science and Engineering, Xiamen University, Xiamen 361005, China (e-mail: meiyang@xmu.edu.cn; yhchen@stu.xmu.edu.cn; lyying@xmu.edu.cn; zwzheng@xmu.edu.cn; longhao@xmu.edu.cn; bzhang@xmu.edu.cn).

Color versions of one or more figures in this article are available at https://doi.org/10.1109/JLT.2021.3053213.

Digital Object Identifier 10.1109/JLT.2021.3053213

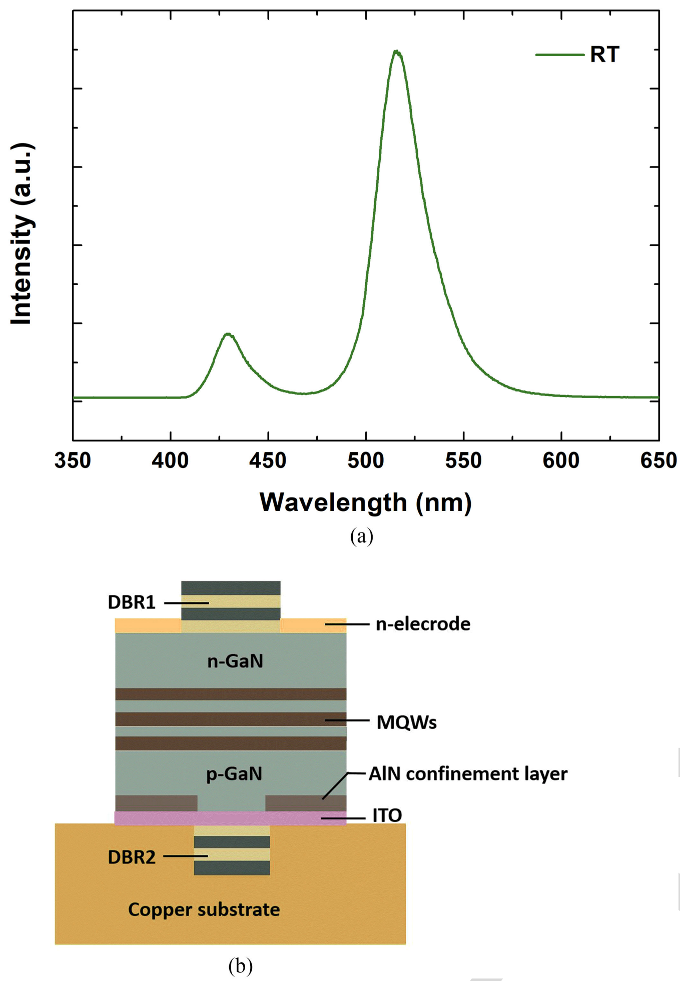

Fig. 1. (a) RT PL spectrum of the epitaxial wafer. (b) Cross-sectional schematic of the fabricated MC light emitter.

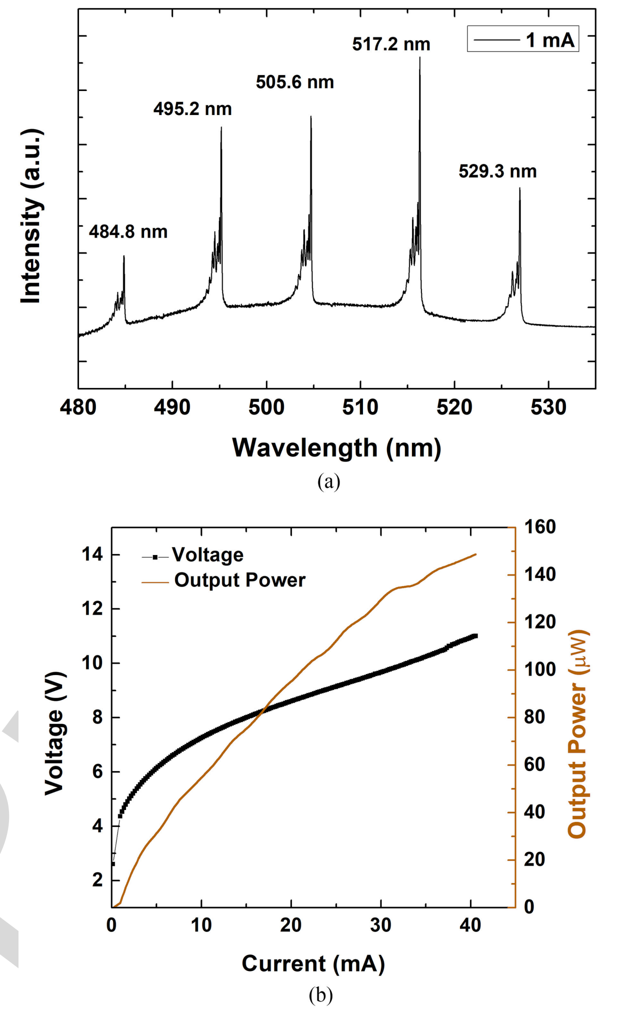

Fig. 2. (a) RT EL spectra of the device measured under 1 mA. (b) L-I-V characteristics of the device.

energy. The optical state density at these distinct energies can be much higher than that of a continuous dispersion. This "photonic dot" effect in this work is promising for the study of CQED at room temperature including the Purcell effect and Bose-Einstein condensation of cavity polaritons.

II. Materials and Methods

The epitaxial wafer was grown on a (0001) c-plane patterned sapphire substrate by metal-organic chemical vapor deposition. The active medium consists of 3 pairs InGaN/GaN pre-well (with low Indium content, ~0.1) and 16 pairs $In_{0.25}Ga_{0.75}N/GaN$ (3/12 nm) QWs. The room-temperature (RT) photoluminescence (PL) spectrum of the epitaxial wafer is shown in Fig. 1(a). The spontaneous emission is centered at around 520 nm, and the small fringe peak at the higher energy comes from the pre-wells with low Indium content. The schematic structure of the device is illustrated in Fig. 1(b). The copper substrate and dual dielectric DBRs structure were realized by substrate transferring and laser lift-off (LLO) techniques, which is similar to our previous reports [29]–[31]. The top and bottom DBRs are 10 and 12.5 pair of TiO_2/SiO_2, respectively. A cylindrical mesa with a diameter of 7 μm was formed on p-GaN and a 60 nm thick sputtered AlN layer was inserted between p-GaN and ITO to laterally confine both optical field and injected current. Together with the dual DBRs, this lateral confinement layer can generate 3D confinement for the optical field, and effectively reduce the lateral optical loss. During device fabrication, the surface roughness of ITO and n-GaN were carefully controlled, and the root-mean-square roughness (RMS) of these cavity edge surfaces are 0.7 and 0.29 nm, respectively. This atomic-level flat cavity surface is essential to reduce scatter loss and guarantee a high cavity Q factor.

III. Results and Discussion

Fig. 2(a) presents the RT electroluminescence (EL) spectra measured from the MC light emitter under 1 mA. The light emission of the device was collected by an objective lens (NA0.35, 10×) and then guided to the spectrometer. Multi-longitudinal mode emission, ranging from 460 to 540 nm, was observed from the spectra due to the relative long cavity length (~3.8 μm) and the broad spontaneous emission spectrum of the QW wafer. The

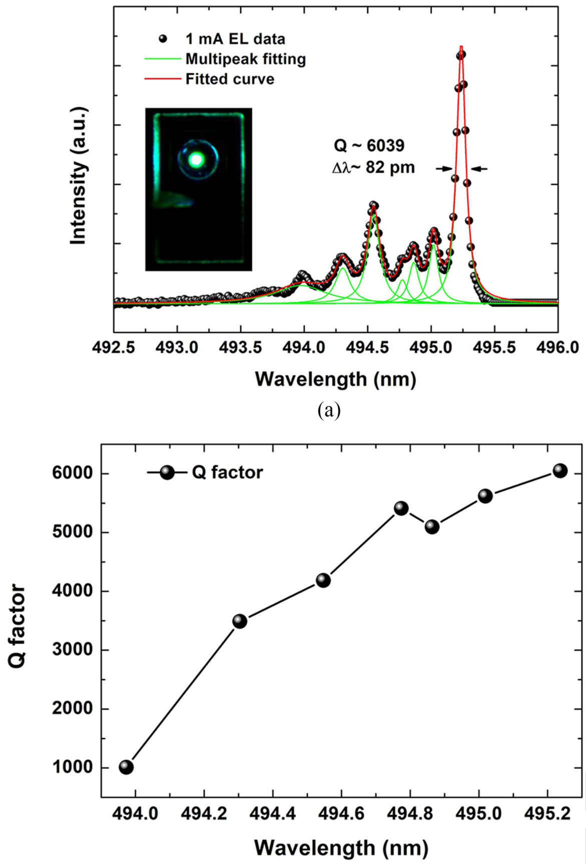

Fig. 3. (a) High resolution spectrum of the 495.25 nm longitudinal mode. (b) Q factor of lateral modes with different mode order.

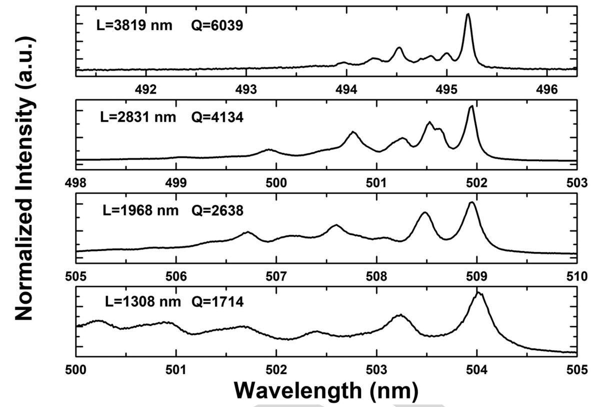

Fig. 4. Emission spectra measured from devices with different cavity length.

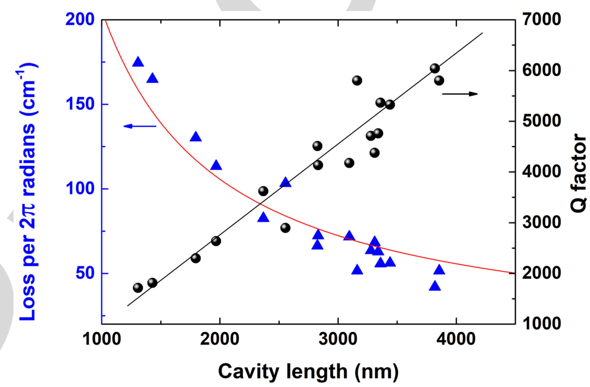

Fig. 5. Cavity Q factor and mode loss per 2π radians as a function of cavity length.

main longitudinal modes of the spectrum located at 484.8, 459.2, 505.6, 517.2, 529.3 nm, respectively. All the longitudinal modes show a multi-peak structure, which comes from the high-order lateral confined modes induced by the index-guiding effect of the buried AlN aperture (refractive index of AlN$\sim$1.98, GaN$\sim$2.40 at 500 nm). The light-current-voltage (L-I-V) characteristic of the device is given in Fig. 2(b). The turn-on voltage is around 6.4 V and the maximum output power is 149 μW under injected current of 40 mA.

The high-resolution spectrum of the 495.2 nm longitudinal mode is shown in Fig. 3(a). More than 7 higher-order lateral confined modes could be recognized and the fundamental mode is featured with the strongest intensity and a linewidth as narrow as 82 pm fitted by Lorentzian function. The Q factor calculated by $\lambda/\Delta\lambda$ is 6039, which is the highest value in electrically injected GaN-based MCs to the best of our knowledge. The high Q factor is attributed to the low loss in the cavity enabled by the high reflective DBRs, atomic level flat cavity end surfaces, and the lateral optical confinement. The effect of these items will be discussed later. The inset of Fig. 3(a) shows the near field emission pattern of the device under 1 mA. The bright emission spot locates pretty well in the center of the aperture, indicating that the injected current and the lateral optical field were effectively confined by the AlN aperture. Fig. 3(b) indicates the Q factors of different order 3D confined modes belongs to the 495.2 nm cavity mode as a function of their emission wavelengths (shorter wavelength corresponds to higher mode order). The Q factor is the highest for the fundamental mode and then decreases with the increase of mode order. This is consistent with the fact that the high-order lateral modes usually located near the edge of confinement aperture, resulting in a larger lateral optical leakage. Also, the diffraction angle of the higher-order modes is larger than the fundamental mode [32], thus more light could penetrate the DBRs and escape from the cavity.

Emission characteristics of devices with different cavity lengths were also investigated. Fig. 4 shows the emission spectra measured from devices with different cavity lengths of 1308, 1968, 2831, and 3819 nm, respectively. Emission from higher-order lateral modes can be clearly observed in all devices, but the linewidth of the fundamental mode decreases with the increase of cavity length. The Q factor of the fundamental emission mode increased from 1714 to 6039 when cavity length was increased from 1038 to 3819 nm. It is also worth to note that the intensity ratio between the fundamental mode and higher-order 3D confined modes is increased, and the latter is suppressed in a longer cavity. This is caused by the increased diffraction loss of higher-order modes which are featured with a larger diffraction angle in a longer cavity. Fig. 5 indicates the experimentally

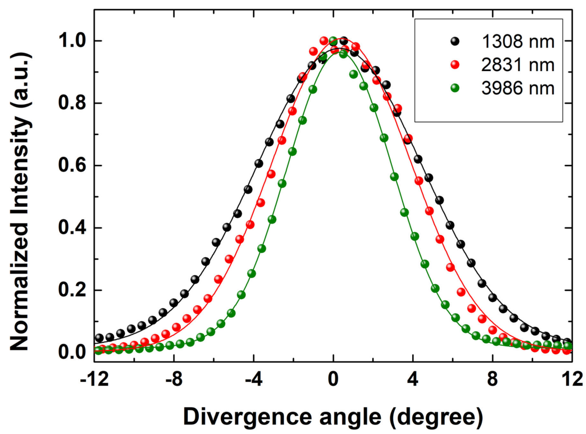

Fig. 6. Far-field image of the fundamental emission mode measured from devices with different cavity lengths.

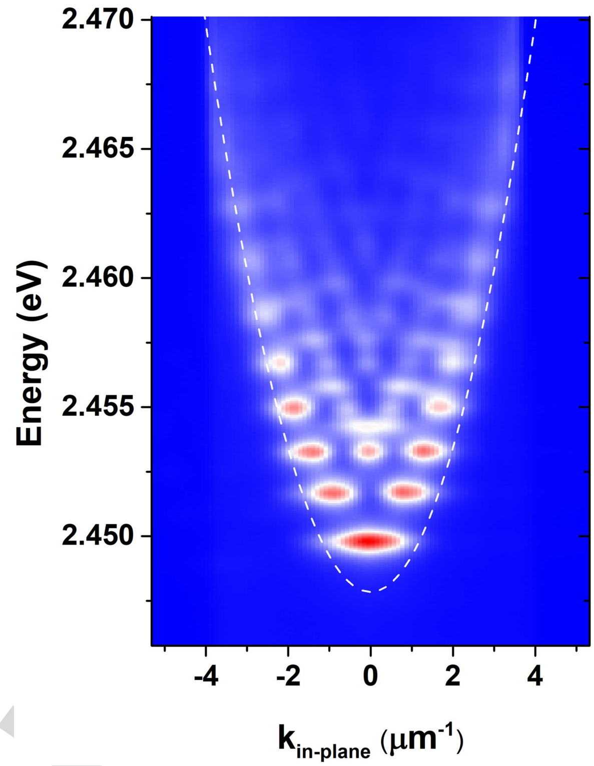

Fig. 7. k space distribution of the 3D confined optical states. The white dashed curve is the calculated mode dispersion in 2D MC without lateral confinement.

measured Q factor of fundamental emission mode, as well as the calculated mode loss per 2π radians as a function of the cavity length. The cavity Q factor increases linearly with the cavity length. This is consistent with the definition of the Q factor, because the mirror loss and scatter loss take place only at the cavity edge surface, and the internal loss can be assumed approximately constant when the optical field propagates inside the cavity. In a longer cavity, the mirror loss and scatter loss are averaged to the total cavity when calculating the mode loss per 2π radians, inducing the decrease of mode loss and increase of Q factor.

In addition to standard spectra measurement, far-field emission characteristics of devices with different cavity lengths are also analyzed by using angle-resolved emission measurement. Fig. 6 shows the far-field image of the fundamental emission mode measured from devices with different cavity lengths of 1308, 2831, and 3986 nm, respectively. The full-width at half-maximum far-field angle of the fundamental modes in these three devices are 9.8°, 8.2°, and 6.3°, respectively. Devices with shorter cavity length exhibit a larger divergence angle. Similar phenomenon has been observed in GaAs based VCSELs [33].

The distribution of 3D confined optical states in the momentum space was also studied through angle-resolved measurement, as shown in Fig. 7. Different from the typical parabolic type continuous mode dispersion in 2D planar MC without lateral confinement (white dashed curve), 3D confined optical states were clearly observed in this work. The dispersion of optical states in k space splits into a series of discrete modes at different energies. The state density of each mode as a function of $k_{in\text{-}plane}$ follows well the simple harmonic oscillator model in a parabolic potential well. This is the first observation and k space measurement of the 3D confined optical states in an electrically injected GaN-based MC. The optical state density at these distinct energies is much higher than that of a continuous dispersion, while there is no state distribution at other energy. This 3D optical confinement in MC with a high Q factor, namely the "photonic dot" effect, can lead to distinctive phenomena, such as the inhibition or acceleration of the spontaneous emission in the so-called weak coupling regime [34], and the Bose-Einstein condensation of cavity polaritons in the strong coupling region [35]. The high cavity Q factor in this work is one sufficient condition to observe these split 3D confined modes and can guarantee more concentrated optical state distribution because of the narrow mode linewidth. At present, only the 3D confined optical states were observed, but the electrically injected high Q factor structure in this work is also eminently suitable for other material systems. We believe that the structure is promising for 3D confined polariton devices working under strong coupling condition, if active layers with narrower exciton emission linewidth and larger exciton binding energy such as thin GaN or AlGaN QWs are utilized.

In the following, the loss mechanism is systematically investigated in the cavity with a high Q factor. The intensity of the light inside the cavity after one round-trip propagation can be given by

$$R_1 R_2 (1 - S_1)\,(1 - S_2) \cdot A\, e^{-\alpha_{inner} \cdot 2d} = A e^{-\alpha_{total} \cdot 2d} \quad (1)$$

where A is the intensity at the starting point, R_1 and R_2 are the reflectivity of DBRs, S_1 and S_2 are the scattering loss at the two end faces of the cavity, α_{inner} is inner absorption coefficient, and d is the cavity length. α_{total} is the effective loss coefficient obtained by converting all loss items into the whole cavity, and can be expressed by

$$\alpha_{total} = \frac{-\ln R_1 R_2}{2d} + \frac{-\ln[(1-S_1)(1-S_2)]}{2d} + \alpha_{inner} \tag{2}$$

with the three items corresponding respectively to leaks and absorption from the DBRs, the scattering loss caused by imperfect morphology of the end face of the cavity, and inner loss originating from the MC layers and lateral optical leakage. Then the expected Q-factor of the cavity can be decomposed into three contributing terms

$$Q^{-1} = Q^{-1}_{DBR} + Q^{-1}_{inner} + Q^{-1}_{scatter} \tag{3}$$

The high Q factor 6039 of the fundamental mode realized in this work could be attributed to the high reflectivity of the dielectric DBRs, the atomic level flat end face of the cavity, the lateral confinement of the optical modes induced by the buried AlN LOC structure, as well as the low loss of GaN layer in the green region. Q^{-1}_{mir} and $Q^{-1}_{scatter}$ could be obtained by

$$Q^{-1}_{mir} = \frac{1}{2\pi} \cdot \frac{-\ln R_1 R_2}{2d} \cdot \frac{\lambda}{n} \tag{4}$$

$$Q^{-1}_{scatter} = \frac{1}{2\pi} \cdot \frac{-\ln[(1-S_1)(1-S_2)]}{2d} \cdot \frac{\lambda}{n} \tag{5}$$

Where λ, n, d are the operating wavelength (495 nm), refractive index (2.39), and cavity length (3819 nm), respectively. The reflectivity is 99.6% and 99.8% for the 10 and 12.5 pair TiO_2/SiO_2 DBRs. The scattering loss S1 (5.468e-5) and S2 (3.781e-4) are calculated by $S_{scatter} = D\{1 - \exp[-(\frac{4\pi\delta}{\lambda})^2]\}$ where δ is the RMS of the cavity end faces (0.29 and 0.76 nm), and D is a calibration coefficient defined as the ratio between the total reflectance of the top DBR versus air and that versus p-GaN [36]. A was calculated to be 1.02 here. Q^{-1}_{mir} and $Q^{-1}_{scatter}$ turned out to be $2.122 \cdot 10^{-5}$ and $1.531 \cdot 10^{-6}$ respectively, i.e., $Q_{DBR} \sim 47094$, $Q_{scatter} \sim 6.532 \cdot 10^5$. These values are much larger than the measured Q factor of 6039, meaning that the loss from the DBRs and surface scattering only occupy a very small part of the total loss in the cavity in our case, due to the high reflectivity of the DBRs and the atomic level flat cavity end face. Q^{-1}_{inner} was calculated to be $\sim 1.427 \cdot 10^{-4}$ i.e., $Q_{inner} \sim 7009$, in the same order of the measured Q value. So, the main loss of the cavity come from the inner loss originating from the absorption of cavity layers, and lateral optical leakage. The inner absorption coefficient α_{inner} was calculated to be 46 cm^{-1} from the equation $Q^{-1}_{inner} = \frac{1}{2\pi} \cdot \alpha_{inner} \cdot \frac{\lambda}{n}$, and mainly consists of three parts including the absorption of GaN layers in the cavity, the absorption due to the ITO layer and the lateral optical loss. The absorption coefficient of doped GaN layer in the green region is $\sim$10 cm^{-1} [37], and the equivalent absorption coefficient of ITO layer was calculated to be ~ 14 cm^{-1} by $\Gamma_r \cdot \alpha_{ITO} \cdot \frac{l}{d}$, where Γ_r ($\sim$1.0 here calculated by transfer matrix method) is the relative gain enhancement factor which is used to express the overlap degree of the ITO layer and standing wave field in the cavity, α_{ITO} is the absorption coefficient of ITO (2000 cm^{-1}) [37], and l is the thickness of ITO layer ($\sim$30 nm) used in this work. Then we obtained that the absorption coefficient caused by the lateral optical loss is $\sim$22 cm^{-1}. This is a relatively small value in GaN-based vertical-cavity structures owing to the lateral optical confinement by the buried AlN LOC structure. Masaru Kuramoto *et al.* reported GaN VCSEL with buried SiO_2 LOC structure and the lateral leakage loss decreased from 73 to 23cm^{-1} when the LOC structure was applied, similar to our results [38]. The use of the AlN layer instead of SiO_2 in this work can improve the thermal dissipation in GaN-based MC with dual dielectric DBRs. The insulation layer in GaN-based MC devices with dual dielectric DBR structure is embedded between p-GaN and substrate. It locates at the main pathway of thermal dissipation from the active region to substrate. In our previous works [39], [40], we found that the SiO_2 LOC layer will degrade device thermal dissipation because of the relatively low thermal conductivity of 1.5 Wm/K. In contrast, AlN has a much higher thermal conductivity of $\sim$200 Wm/K, Therefore, using AlN will enable us to improve thermal dissipation inside the device. But it needs to be noted that lasing action was not realized in this work although a 3D confined low loss cavity with a high Q factor was fabricated. At present, green VCSEL is still difficult based on c-plane InGaN QWs grown on the sapphire substrate because of the "green gap", which is caused by the large quantum confined stark effect and low emission efficiency in the green region [30], [42]. The material gain of c-plane green InGaN QWs still needs further optimization to realize lasing action.

IV. Conclusions

In summary, we have demonstrated an electrically injected green GaN-based MC light emitter with a high Q factor of 6039 which is the highest value in electrically injected GaN-based MC light emitters to the best of our knowledge. The MC light emitter is featured with dual dielectric DBRs and an AlN buried LOC structure. The emission characteristics as a function of cavity length, as well as the loss mechanism in the cavity, were systematically analyzed. The high Q factor was contributed to the high reflectivity of DBRs, low scattering loss of the cavity end face, as well as the small lateral optical leakage induced by the LOC structure. The 3D confined optical states inside the cavity were also observed and studied through angle-resolved measurement. This electrically injected 3D confined GaN-based MC light emitter with a high Q factor is promising for the study of CQED at room temperature including Purcell effect and Bose-Einstein condensation of cavity polaritons.

References

[1] S. John, "Strong localization of photons in certain disordered dielectric superlattices," *Phys. Rev. Lett.,* vol. 58, no. 23, pp. 2486–2489, Jun. 1987.

[2] T. Asano, B.-S. Song, Y. Akahane, and S. Noda, "Ultrahigh-Q nanocavities in two-dimensional photonic crystal slabs," *IEEE J. Sel. Top. Quantum Electron.,* vol. 12, no. 6, pp. 1123–1134, Nov./Dec. 2006.

[3] S. T. Jagsch *et al.*, "A quantum optical study of thresholdless lasing features in high-beta nitride nanobeam cavities," *Nat. Commun.*, vol. 9, no. 1, p. 564, Feb. 2018.

[4] I. Roland *et al.*, "Near-infrared III-nitride-on-silicon nanophotonic platform with microdisk resonators," *Opt Exp.,* vol. 24, no. 9, pp. 9602–9610, May 2016.

[5] P. Michler *et al.*, "A quantum dot single-photon turnstile device," *Science,* vol. 290, pp. 2282–2285, 2000.

Q2 [6] G. Christmann, R. Butté, E. Feltin, J.-F. Carlin, and N. Grandjean, "Room temperature polariton lasing in a GaN/AlGaN multiple quantum well microcavity," *Appl. Phys. Lett.,* vol. 93, no. 5, 2008.

[7] S. Nakamura, T. Mukai, and M. Senoh, "Candela-class high-brightness InGaN/AlGaN double-heterostructure blue-light-emitting diodes," *Appl. Phys. Lett.,* vol. 64, no. 13, pp. 1687–1689, 1994.

[8] D. Sanvitto and S. Kena-Cohen, "The road towards polaritonic devices," *Nat. Mater.,* vol. 15, no. 10, pp. 1061–1073, Oct. 2016.

[9] D. Miller, "Device requirements for optical interconnects to silicon chips," *Proc. IEEE,* vol. 97, no. 7, pp. 1166–1185, 2009.

[10] A. Di Falco, L. O'Faolain, and T. F. Krauss, "Chemical sensing in slotted photonic crystal heterostructure cavities," *Appl. Phys. Lett.,* vol. 94, no. 6, 2009.

[11] A. Bhattacharya, M. Z. Baten, I. Iorsh, T. Frost, A. Kavokin, and P. Bhattacharya, "Room-temperature spin polariton diode laser," *Phys. Rev. Lett.*, vol. 119, no. 6, Aug. 2017, Art. no. 067701.

[12] G. C. Raphaël Butté *et al.*, "Room temperature polariton lasing in III-nitride microcavities: A comparison with blue GaN-based vertical cavity surface emitting lasers," in *Proc. SPIE*, San Jose, CA, USA, 2009.

[13] R. Tao, K. Kamide, M. Arita, S. Kako, and Y. Arakawa, "Room-temperature observation of trapped exciton-polariton emission in GaN/AlGaN microcavities with air-gap/III-nitride distributed bragg reflectors," *ACS Photon.,* vol. 3, no. 7, pp. 1182–1187, 2016.

[14] R. Butté and N. Grandjean, "III-nitride photonic cavities," *Nanophotonics,* vol. 9, no. 3, pp. 569–598, 2020.

[15] K. J. Vahala, "Optical microcavities," *Nature,* vol. 424, no. 14 , pp. 839–846, Aug. 2003.

[16] Ž. Gačević *et al.*, "Q-factor of (In,Ga)N containing III-nitride microcavity grown by multiple deposition techniques," *J. Appl. Phys.,* vol. 114, no. 23, 2013.

[17] G. Christmann, D. Simeonov, R. Butté, E. Feltin, J. F. Carlin, and N. Grandjean, "Impact of disorder on high quality factor III-V nitride microcavities," *Appl. Phys. Lett.,* vol. 89, no. 26, 2006, doi: 10.1063/1.2420788.

[18] R. T. Munetaka Arita, Satoshi Kako, Yasuhiko Arakawa, "Structural and optical characterization of high-quality vertical microcavities with free-standing III-nitride thin films," *第74回応用物理学会秋季学術講演会 講演予稿集*, vol. 16p-B5-11,

Q3 pp. 15–079, 2013.

[19] M. Arita, S. Kako, S. Iwamoto, and Y. Arakawa, "Fabrication of AlGaN two-dimensional photonic crystal nanocavities by selective thermal decomposition of GaN," *Appl. Phys. Exp.,* vol. 5, no. 12, 2012.

[20] N. V. Trivino, R. Butte, J. F. Carlin, and N. Grandjean, "Continuous wave blue lasing in III-nitride nanobeam cavity on silicon," *Nano. Lett.,* vol. 15, no. 2, pp. 1259–1263, Feb. 2015.

[21] S. S. M. Mexis *et al.*, "High quality factor nitride-based optical cavities microdisks with embedded GaN Al(Ga)N quantum dots," *Opt. Lett.* vol. 36, no. 12, pp. 2203–2205, 2011.

[22] I. Rousseau, G. Callsen, G. Jacopin, J.-F. Carlin, R. Butté, and N. Grandjean, "Optical absorption and oxygen passivation of surface states in III-nitride photonic devices," *J. Appl. Phys.,* vol. 123, no. 11, 2018.

[23] W. J. Liu, X. L. Hu, L. Y. Ying, J. Y. Zhang, and B.-P. Zhang, "Room temperature continuous wave lasing of electrically injected GaN-based vertical cavity surface emitting lasers," *Appl. Phys. Lett.,* vol. 104, no. 25, 2014.

[24] H. M. Hideki Matsubara, H. S., Y. Jianglin, Y. Jianglin, Yue Jianglin, "GaN photonic-crystal surface-emitting laser at blue-violet wavelengths," *Science,* vol. 319, no. 5862, pp. 445–447, 2019.

[25] M. Feng *et al.*, "Room-temperature electrically pumped InGaN-based microdisk laser grown on Si," *Opt Exp.,* vol. 26, no. 4, pp. 5043–5051, Feb. 2018.

[26] F. Tabataba-Vakili *et al.*, "III-nitride on silicon electrically injected microrings for nanophotonic circuits," *Opt Exp.,* vol. 27, no. 8, pp. 11800–11808, Apr. 2019.

[27] M. Kneissl, M. Teepe, N. Miyashita, N. M. Johnson, G. D. Chern, and R. K. Chang, "Current-injection spiral-shaped microcavity disk laser diodes with unidirectional emission," *Appl. Phys. Lett.,* vol. 84, no. 14, pp. 2485–2487, 2004.

[28] C. S. M. Kuramoto, N. Futagawa, M. Nido, M. Nido, "Reduction of internal loss and threshold current in a laser diode with a ridge by selective regrowth (RiS-LD)," *Physica Status Solidi,* vol. 192, no. 2, pp. 329–334, 2002.

[29] Y. Mei *et al.*, "Tunable InGaN quantum dot microcavity light emitters with 129 nm tuning range from yellow-green to violet," *Appl. Phys. Lett.,* vol. 111, no. 12, 2017.

[30] Y. Mei *et al.*, "Quantum dot vertical-cavity surface-emitting lasers covering the 'green gap'," *Light Sci. Appl.,* vol. 6, no. 1, Jan 2017, Paper. e16199.

[31] R. Xu *et al.*, "Green vertical-cavity surface-emitting lasers based on combination of blue-emitting quantum wells and cavity-enhanced recombination," *IEEE Trans. Electron. Devices,* vol. 65, no. 10, pp. 4401–4406, Oct. 2018.

[32] H. Nakajima *et al.*, "Single transverse mode operation of GaN-based vertical-cavity surface-emitting laser with monolithically incorporated curved mirror," *Appl. Phys. Exp.,* vol. 12, no. 8, 2019.

[33] H. J. Unold, S. W. Z. Mahmoud, R. Jäger, M. Kicherer, M. C. Riedl, and K. J. Ebeling, "Improving single-mode VCSEL performance by introducing a long monolithic cavity," *IEEE Photon. Technol. Lett.,* vol. 12, no. 8, pp. 939–941, Aug. 2000.

[34] M. Bayer, A. Forchel, T. L. Reinecke, P. Knipp, and S. Rudin, "Confinement of light in microresonators for controlling light–matter interaction," *Physica Status Solidi,* vol. 191, no. 1, pp. 3–32, 2002.

[35] G. Roumpos, W. H. Nitsche, S. Höfling, A. Forchel, and Y. Yamamoto, "Gain-induced trapping of microcavity exciton polariton condensates," *Phys. Rev. Lett.,* vol. 104, no. 12, 2010, Art. no. 126403.

[36] W.-J. Liu *et al.*, "Low threshold lasing of GaN-based VCSELs with sub-nanometer roughness polishing," *IEEE Photon. Technol. Lett.,* vol. 25, no. 20, pp. 2014–2017, Oct. 2013.

[37] J. T. Leonard *et al.*, "Demonstration of a III-nitride vertical-cavity surface-emitting laser with a III-nitride tunnel junction intracavity contact," *Appl. Phys. Lett.,* vol. 107, no. 9, 2015.

[38] M. Kuramoto *et al.*, "Enhancement of slope efficiency and output power in GaN-based vertical-cavity surface-emitting lasers with a SiO_2-buried lateral index guide," *Appl. Phys. Lett.,* vol. 112, no. 11, 2018.

[39] Y.-H. Chen *et al.*, "Improvement of thermal dissipation of GaN-based micro cavity light-emitting devices," *IEEE Photon. Technol. Lett.,* vol. 33, no. 1, pp. 1–1, Jan. 2021.

[40] Y. Mei *et al.*, "A comparative study of thermal characteristics of GaN-based VCSELs with three different typical structures," *Semicond. Sci. Technol.,* vol. 33, no. 1, 2018.

[41] S. Hang *et al.*, "On the origin for the hole confinement into apertures for GaN-based VCSELs with buried dielectric insulators," *Opt. Exp.,* vol. 28, no. 6, pp. 8668–8679, Mar. 2020.

[42] T. Hamaguchi *et al.*, "Room-temperature continuous-wave operation of green vertical-cavity surface-emitting lasers with a curved mirror fabricated on {20−21} semi-polar GaN," *Appl. Phys. Exp.,* vol. 13, no. 4, 2020.

Yang Mei was born in Henan, China, in 1994. He received the B.S. degree in physics from the China University of Geoscience, Wuhan, China, in 2014 and the Ph.D. degree from Xiamen University, Xiamen, China, in 2020. He is currently an Assistant Professor with the College of Electronic Science and Technology, Xiamen University, where he is engaged in wide gap semiconductor materials and devices, especially GaN-based microcavities and vertical-cavity surface-emitting lasers.

Yan-Hui Chen, biography not available at the time of publication.

Lei-Ying Ying was born in Guangzhou, China, in 1963. She received the B.S. degree in physics from Zhongshan University, Guangzhou, China, and the M.E. degree in electronic engineering from Hebei Semiconductor Research Institute, Shijiazhuang, China, in 1986. In 2011, she joined the Department of Physics, Xiamen University, Xiamen, China, where she is currently an Engineer of semiconductor devices. Her current research interests include microfabrication or nanofabrication and semiconductor devices for optoelectronic applications.

Zhi-Wei Zheng received the Ph.D. degree in microelectronics from the Institute of Microelectronics, Chinese Academy of Sciences, Beijing, China, in 2014. He is currently an Associate Professor with the School of Electronic Science and Engineering, Xiamen University, Xiamen, China. His research interests include semiconductor materials and devices for electronic and optoelectronic applications.

Hao Long was born in JiangXi Province, China, in 1986. He received the B.S. and Doctor degrees in physics from Peking University, Beijing, China, in 2008 and 2013, respectively. From 2013 to 2015, he was a Staff Researcher at Lenovo Inc., Beijing, China, for emerging display development. In 2015, he joined the Department of Electrical Engineering, Xiamen University, Xiamen, China, as a Postdoctor. He is currently an Associate Professor with Xiamen University. He is working toward the research and development of wide bandgap semiconductor (III-nitride and Ga_2O_3) material growth, device fabrication and characterization, and fundamental light-matter interaction in semiconductor micro-cavities.

Bao-Ping Zhang was born in Hebei, China, in 1963. He received the B.S. degree in physics from Lanzhou University, Lanzhou, China, in 1983, the M.E. degree in electronic engineering from Hebei Semiconductor Research Institute, Shijiazhuang, China, and the Dr. Eng. degree in applied physics from The University of Tokyo, Tokyo, Japan, in 1994. He is currently a Distinguished Professor with the College of Electronic Science and Technology, Xiamen University, China, where he is engaged in wide gap semiconductor materials and devices, especially GaN-based LEDs and vertical-cavity surface-emitting lasers.